A study of the bioactivity, hemocompatibility and antimicrobial properties of a zinc oxide and calcium phosphate composite for bone regeneration

A. A. Barbosa[1]*, S. A. Júnior[2], A. V. Ferraz[1]
[1]Federal University of San Francisco Valley, Av. Antonio Carlos Magalhães 310, Juazeiro, BA, Brazil
[2]Federal University of Pernambuco, Recife, PE, Brazil

Abstract

The need for the reconstruction of large bone defects is an issue that arouses great interest in the field of materials science. The development of synthetic grafts similar to bone tissue is a promising option. Thus, this study proposes the synthesis of a zinc oxide and calcium phosphate composite in order to evaluate both its properties and its potential for bone applications. The synthesis of the HAp/TCP@ZnO composite was carried out in two stages; first, the precipitation method was employed. In the second stage, the ZnO was incorporated into the powder produced in the first stage. After the characterization of the material, the presence of HAp in its X-ray diffractogram as the major phase and TCP as the secondary phase was verified; moreover, ZnO peaks were also detected. Tests in a simulated body fluid indicated that the composite was highly bioactive, whereas hemolysis tests confirmed its non-toxicity. The addition of 10.0% of ZnO to the biomaterial provided it with antimicrobial properties.
Keywords: biomaterial, hydroxyapatite, antimicrobial, tricalcium phosphate, non-toxic.

INTRODUCTION

A high number of orthopedic surgeries are performed worldwide every year. It is estimated that 22.3 million procedures occurred in 2017 and that this amount could achieve approximately 28.3 million by 2022 [1]. On the other hand, it is known that, although bones can regenerate, such ability is limited when major defects resulting from trauma or disease are involved. Thus, a huge demand for biomaterials that work as bone substitutes has been observed [2]. The graft that comprehends the best conditions for bone regeneration, used in both the medical and dental fields, is the autologous bone graft, which is harvested from the individual themselves. It allows the transplantation of osteogenic cells, does not generate an immune reaction, and allows quick recovery of bone tissue [3]. However, the amount of autologous graft is generally limited; moreover, a longer surgery time is usual, as well as the occurrence of morbidities at the donor site such as bruises, infections, and severe pain, which restricts its use [4, 5]. In addition to autografts, allogeneic grafts are also a frequent choice. They usually consist of cadavers and the major restriction to their use is their high risk of disease transmission. To help mitigate this risk, allografts undergo several treatments that reduce the original biological and mechanical properties of the material [6]. Therefore, the need for repairing large bone defects is an issue that arouses great interest in the field of materials science. The development of synthetic grafts similar to bone tissue is a promising option. On the other hand, in addition to being cost-effective, synthetic materials that are candidates for bone substitutes must gather several properties such as biocompatibility, osteoconductivity, bioresorption, and structural similarity [7].

The synthetic materials that are most similar to bone tissue are calcium phosphate ceramics. The hydroxyapatite (HAp), $Ca_{10}(PO_4)_6(OH)_2$, is an example; its chemical composition and *in vivo* behavior resemble those of the natural HAp that is found in bones. However, this ceramic presents low resorption rates and, consequently, a slower integration with the host bone [8]. The tricalcium phosphate (TCP), $Ca_3(PO_4)_2$, is another example. TCP has different phases, α-TCP and β-TCP, with the latter presenting high solubility and a high degradation rate, in addition to an elevated resorption rate when compared to HAp [9]. Another material that stands out in the study of bone substitutes is zinc (Zn). According to the literature, the presence of Zn in materials used as grafts or prostheses increases bone formation [10, 11]. As for zinc oxide (ZnO), it presents, in its nanometric form, antimicrobial activity against several bacterial species and, therefore, may help prevent grafting-related infections [12]. Hence, this study developed a composite biomaterial made of HAp, TCP, and ZnO in order to evaluate both its properties and its potential to be a bone substitute.

MATERIALS AND METHODS

HAp/TCP synthesis: the biphasic HAp/TCP biomaterial was prepared following the methodology described in the literature for pure HAp [13]. We used calcium sulfate hemihydrate ($CaSO_4.½H_2O$) solutions (Ind. Gesso Mineral), ammonium phosphate dibasic [$(NH_4)_2HPO_4$, 98%, Vetec], and ammonia solution (NH_4OH, R.G., Exodo Cient.). The

**amanda.barbosa@univasf.edu.br*
https://orcid.org/0000-0003-0266-4604

precipitation method was used in the synthesis. In short, the $(NH_4)_2HPO_4$ solution was added (20 mL.min^{-1}) to the $CaSO_4.½H_2O$ under agitation, maintaining the stoichiometric ratio Ca/P=1.66. During the synthesis, the pH of the medium was kept at around 8.0 by adding an NH_4OH 3.0 mol.L^{-1} solution. After 1.0 h of agitation and, afterward, 48.0 h of rest, the precipitate obtained was filtered, washed with deionized water until neutral pH, and oven-dried at 100 ºC for 24.0 h.

Synthesis of the HAp/TCP@ZnO composite: for the synthesis of the composite, the methodology described in the literature [14] was followed with some modifications. Initially, a suspension of ZnO nanoparticles (NPs, Synth) in the form of a fine powder with particles smaller than 100 nm, was prepared using 20.0 mL of deionized water and 10.0 mL of glycerin (R.G., Proquímios) to obtain a viscous medium capable of avoiding the precipitation of the ZnO particles (ZnO fractions: 0.0, 5.0%, and 10.0%). The mixture remained under magnetic agitation (200 rpm) and heating (90 ºC) until solubilization. Then, 1.0 g of the HAp/TCP powder obtained in the previous stage was added to the medium under agitation for 10 min. Later, the material was oven-dried for 24.0 h at 100 ºC and then calcined at 900 ºC for 3.0 h (10 ºC.min^{-1}), resulting in HAp/TCP@ZnO.

Antimicrobial assay: the antimicrobial activity of ZnO in the HAp/TCP@ZnO composite was evaluated from the potential formation of inhibition zones against Staphylococcus aureus (S. aureus) ATCC 25923 bacteria, the most frequent microorganism in surgical infections [15]. To perform the assay, bacterial cultures (stock solution) were cultivated on agar at 4 ºC; then, isolated colonies were selected to form 0.5 McFarland turbidity. The plating was carried out using 10 µL of the resulting solution, where bacteria were inoculated in 150 mm plates with Mueller-Hinton agar to stimulate microbial growth. Then, pellets (50 mg and 6.0 mm diameter) obtained by pressing the different samples in powder form (0.0, 5.0%, and 10.0% ZnO) were aseptically deposited on the surface of the plates. The resulting plates were incubated at 37 ºC for 24 h and, after that, it was possible to observe the potential formation of growth inhibition zones around each sample, which were recorded photographically.

Bioactivity test: the chemical activity of the composite was assessed from its interaction with a simulated body fluid (SBF), following Kokubo and Takadama [16]. This solution was prepared with an ionic concentration similar to that of blood plasma, namely: sodium chloride (NaCl), sodium hydrogencarbonate ($NaHCO_3$), potassium chloride (KCl), dipotassium hydrogen phosphate trihydrate ($K_2HPO_4.3H_2O$), magnesium chloride hexahydrate ($MgCl_2.6H_2O$), calcium chloride ($CaCl_2$), sodium sulfate (Na_2SO_4), tris(hydroxymethyl) aminomethane [$(HOCH_2)_3CNH_2$], and hydrochloric acid (HCl); all analytic reagents (Vetec Quim. Fina). The assay was performed using a volume three times the minimum recommended for each sample. Samples in the form of pellets (50 mg and 6.0 mm diameter) were submerged in SBF. The study was carried out considering different periods (0 to 21 days) and the samples were kept under constant agitation and a constant temperature of 37 ºC. During the entire test, the solutions were renewed every 3 days, and, at the end of each period, the pellets were washed with deionized water, oven-dried at 40 ºC and then stored for characterization.

In vitro hemocompatibility test: in order to evaluate the hemocompatibility of the HAp/TCP@ZnO composite, three different concentrations (100, 500, and 1000 µg.mL^{-1}) were analyzed. The solutions were prepared using a saline solution (Needs) as solvent. For this assay, 2.0 mL of blood was collected via cardiac puncture of a Swiss mouse anesthetized with ketamine (150 mg.kg^{-1}) and xylazine (15 mg.kg^{-1}). The blood obtained was immediately mixed with an anticoagulant (EDTA solution, Doles) and, later, solubilized in 10.0 mL of saline solution and centrifuged for 4 min at 3000 rpm to remove the plasma. Then, a red blood cell solution at 1.0% was prepared using saline solution. For every 1.0 mL of this solution, 1.0 mL of the solution being studied was added in triplicates. The tubes containing the mixtures were agitated at 100 rpm for 1 h and then centrifuged for 4 min at 3000 rpm. Using a spectrophotometer, the amount of hemoglobin released in the supernatant was quantified at λ=540 nm and the degree of hemolysis was calculated. Both positive and negative controls were prepared using a 0.1% Triton X-100 solution (Sigma-Aldrich) and saline solution, respectively. The experimental protocols were approved by the Animal Ethics Committee of the Federal University of São Francisco Valley (UNIVASF).

Characterization: the crystalline phases presented in the HAp/TCP@ZnO composite were analyzed via X-ray diffraction (XRD, Diffract ACT Series 1000, Siemens), using the Kα line of copper (λ=1.54056 Å) at 40 kV and 40 mA. The 2θ range was from 10º to 60º, with a step size of 0.02º and a measuring time of 1 s per step. Phase identification was confirmed using the X'Pert HighScore Plus 2.0a software. The experimental XRD pattern was compared with the parameters of the ICSD 16742 reference file, corresponding to HAp [$Ca_{10}(PO_4)_6(OH)_2$], belonging to the hexagonal crystal system and to the P63/m space group, and the ICSD 6191 reference file, corresponding to tricalcium phosphate [TCP, $Ca_3(PO_4)_2$], belonging to the rhombohedral crystal family and to the R3c space group. The morphology of the samples was observed using a scanning electron microscope (SEM, TM1000, Hitachi, and Vega 3, Tescan). The samples were coated with a thin layer of gold (metalizing process) to enhance surface conductivity. The functional groups present in the composite material were also observed from the analysis of their spectra within the infrared region obtained by the Fourier-transform infrared spectroscopy (FTIR, Spectrum Two, PerkinElmer) for a wavelength range of 4000-400 cm^{-1}. The samples were prepared by the KBr pellet method using mechanical pressing.

RESULTS AND DISCUSSION

The composite produced was initially assessed regarding its antimicrobial activity provided by the action of ZnO. In this case, Fig. 1 shows a photographic image taken after the incubation period of the materials with Gram-positive bacteria S. aureus, whereas Table I identifies the respective

samples. The formation of inhibition zones around the pellets is indicative of the antiproliferative activity of bacteria [17]. Samples with 0% ZnO work as the negative control in this assay since no antimicrobial effect is expected from them. This hypothesis was confirmed by the test, given that no inhibition zones were formed around pellets 1 and 2, as indicated in both Fig. 1 and Table I. The addition of 5.0% ZnO led to inconclusive results, given that 2 out of 3 samples (no. 3 and no. 5, Table I) did not form inhibition zones, whereas pellet no. 4 displayed a slight inhibition. On the other hand, an effective antimicrobial activity was confirmed for pellets 6, 7, and 8, which had 10% ZnO in their composition; these presented halos with a mean size of 7.3±0.6 mm, and thus, this sample was chosen for subsequent tests and characterizations. These data corroborated the one observed by Narayanan et al. [18] who found an increasing bacterial inhibition due to the higher concentration of ZnO NPs. In this case, inhibition halos with 18 and 20 mm were obtained for concentrations of 20% and 40% of ZnO, respectively, against the bacteria S. aureus. Albukhaty et al. [19] obtained the formation of inhibition halos with 16 and 27 mm for concentrations of 20% and 40% of ZnO and bacteria S. aureus. It is noteworthy that one of the main mechanisms of action responsible for the antibacterial effect of ZnO NPs is attributed to the oxidative stress caused in the bacterial membrane. This occurs due to the interaction of reactive oxygen species (ROS) generated by metallic oxides that damage the cell leading to death [20].

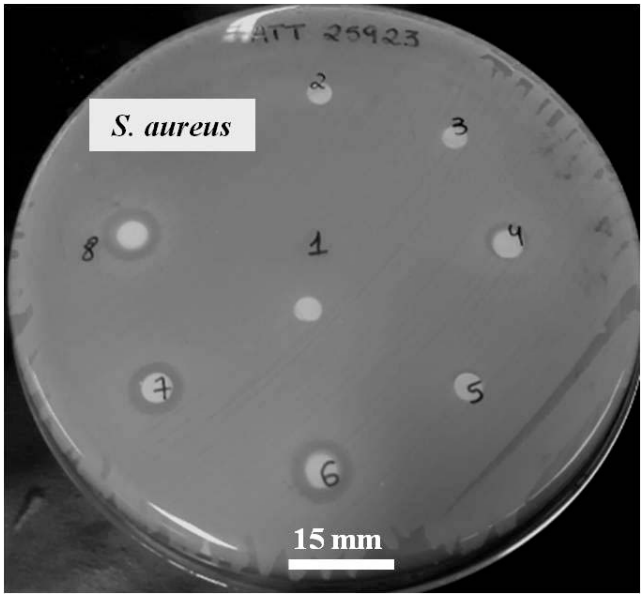

Figure 1: Image of the plate with samples of the composite material after incubation at 35 ºC/24 h with Staphylococcus aureus showing the inhibition zones formed.

Table I - Sample identification (Fig. 1) and formation of inhibition zones in bacteria.

Sample	ZnO (%)	Antibacterial activity (S. aureus)
1	0	No
2	0	No
3	5	No
4	5	Yes
5	5	No
6	10	Yes
7	10	Yes
8	10	Yes

Fig. 2a (ii) presents the FTIR spectrum for the calcium phosphate composite with 10% ZnO, which presented the best antimicrobial response. In this composite, the characteristic absorption bands of HAp can be observed in the vibrations at: 569 and 609 cm^{-1} attributed to the deformation ν_4 O-P-O in PO_4^{3-} or ν_4 O-P-O in HPO_4^{2-}; 954 to 956 cm^{-1} for ν_1 symmetric elongation PO_4^{3-}; 1032 to 1100 cm^{-1} for ν_3 asymmetric stretch of PO_4^{3-} or ν_6 PO_3 stretch in HPO_4^{2-}; a very characteristic band for HAp at 3580 cm^{-1} attributed to ν_5 hydroxyl O-H stretching [21], as well as

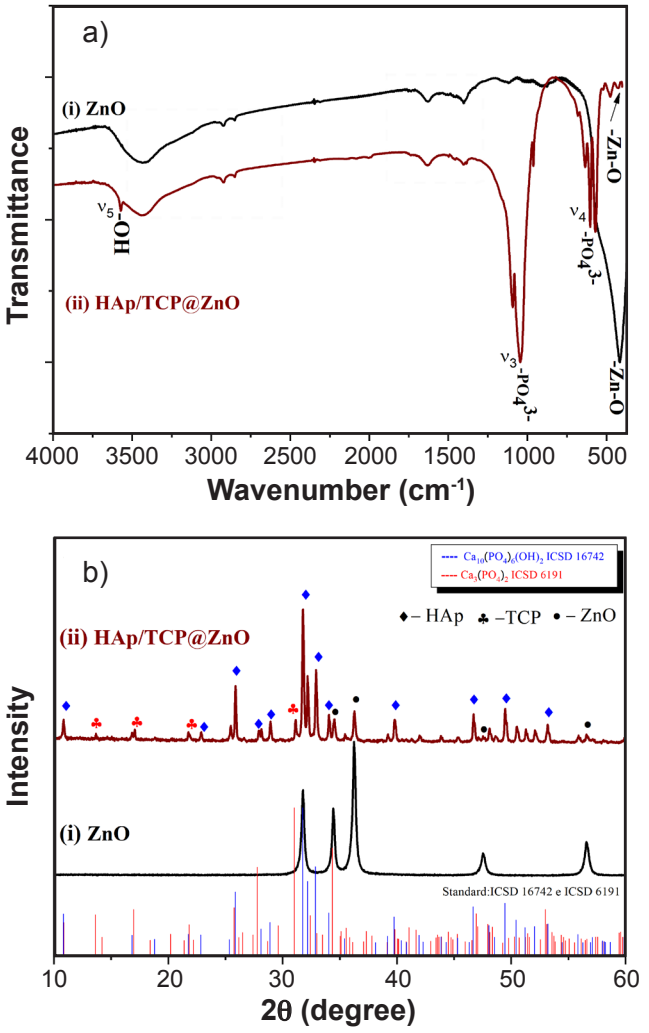

Figure 2: FTIR spectra (a) and X-ray diffractograms (b) of: i) ZnO; and ii) HAp/TCP@10%ZnO.

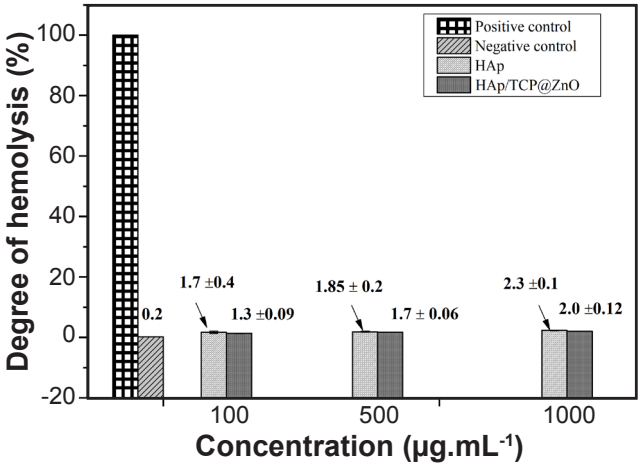

Figure 3: Results for *in vitro* hemocompatibility for HAp and HAp/TCP@10%ZnO.

the presence of low-intensity bands corresponding to ZnO - these can be compared with the ZnO spectrum shown in Fig. 2a (i), where the typical ZnO absorption band was noticed at 429 cm^{-1}. Low-intensity bands were detected at 1392, 1623, 2921, and 3431 cm^{-1} in both spectra and corresponded to the OH and C=O groups, usually due to humidity and CO_2 in the air [22]. In order to identify the crystalline phases of the calcium phosphates present in the composite, XRD analyses were performed. In Fig. 2b (ii) we can see that hexagonal HAp in the P63/m space group is the major phase of the composite, in accordance with the ICSD 16742 file; however, peaks of lower intensity were attributed to the secondary phase TCP, ICSD 6191. The presence of ZnO on the surface of the composite particles was confirmed by the peaks at 2θ 34.55º (002), 36.37º (101), 47.45º (102), and 56.62º (110) attributed to the hexagonal phase of ZnO according to ICSD 57450 [23] and compatible with the peaks observed in the diffractogram of pure ZnO, Fig. 2b (i). Thus, the analyses here performed confirmed HAp as the major phase of the material under study, TCP as the secondary phase, and ZnO NPs scattered throughout the material.

The hemolysis assay is of major importance to assess the interaction between a biomaterial and blood; hence, the *in vitro* degree of hemolysis of the composite is presented in Fig. 3. From the results obtained, we verify that the hemolysis values increased as the concentration of the solutions increased and ranged from 1.3% to 2.0% for HAp/TCP@ZnO and 1.7% to 2.3% for pure HAp, used for comparison. Thus, considering the ASTM 756 (American Society for Testing and Materials) classification for the degree of hemolysis (<2.0% non-hemolytic; 2.0% to 5.0% slightly hemolytic; and >5.0% hemolytic [24]), we concluded that the composite is a hemocompatible material at the concentrations tested. This conclusion corroborated results found in the literature such as Tank et al. [25], who tested HAp doped with different Zn concentrations (2.0%, 5.0%, and 10.0%) using human blood and obtained a degree of hemolysis lower than 2.0%, while Bandgar et al. [26] studied the hemocompatibility of HAp and HAp doped with Cr^{3+} ions and verified a degree of hemolysis of 1.0% for pure HAp and 1.8% to 4.6% for HAp doped with increasing percentages of chromium.

Fig. 4 shows the morphology of the HAp/TCP@ZnO composite, where it is possible to see that the size of the particles was nanometric and they were round and elongated. The larger particles, as well as the agglomerates observed, can be attributed to the beginning of the sintering process of the sample due to the high calcination temperature. In the micrograph of Fig. 4b, it is also possible to verify the presence of several pores in the material. Moreover, the use of ZnO NPs to coat the HAp/TCP particles was homogeneous since no differences were observed on the surfaces of the particles.

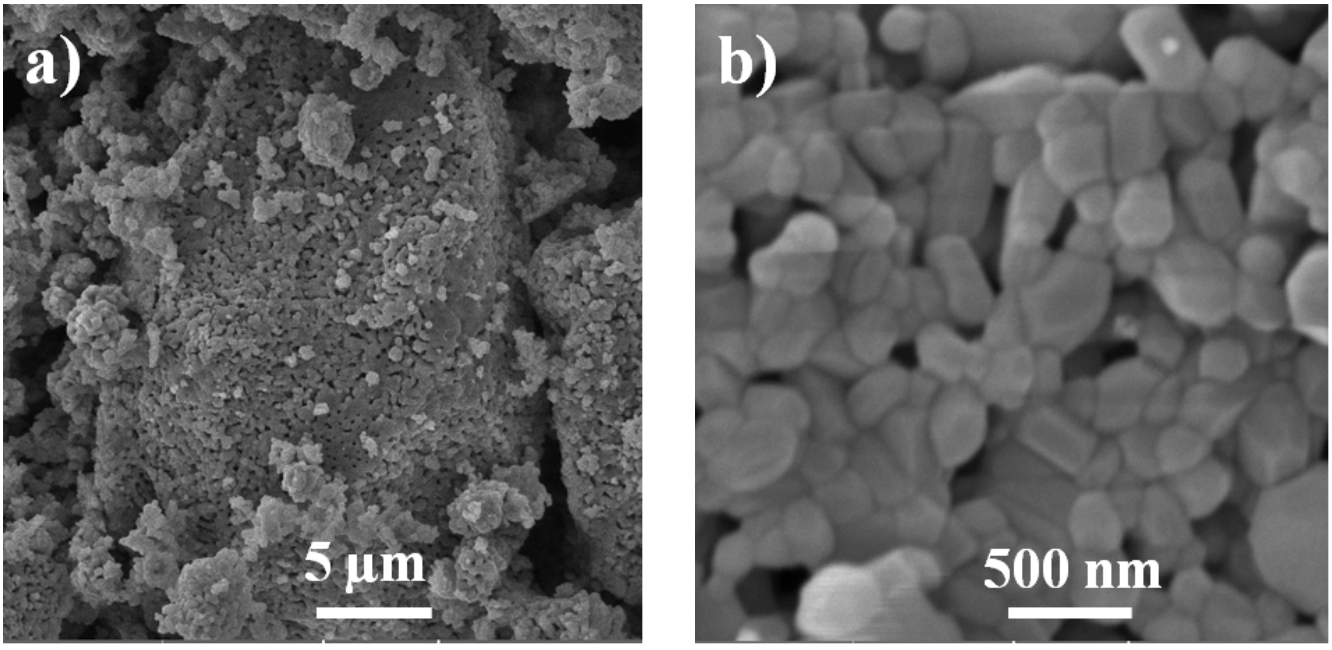

Figure 4: SEM micrographs of the HAp/TCP@10%ZnO composite.

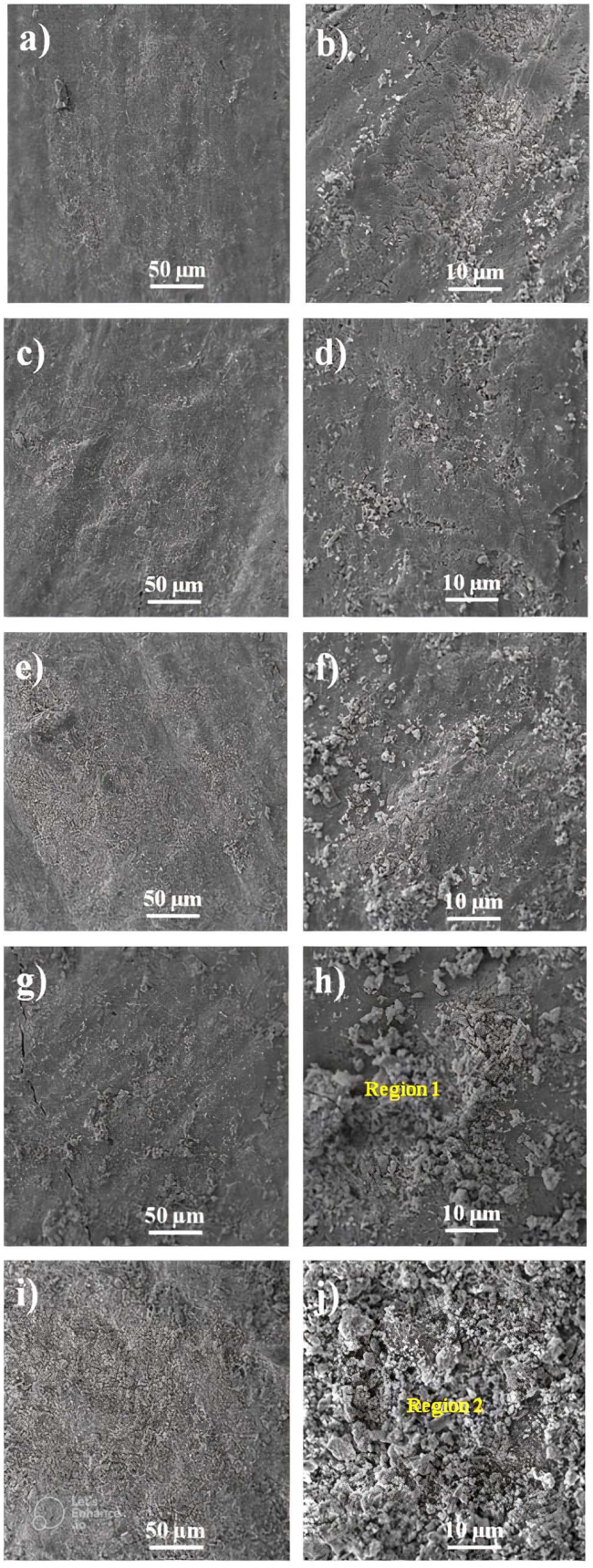

Figure 5: SEM micrographs of the surface of HAp/TCP@10%ZnO pellets after different immersion times in SBF at 37 ºC and pH=7.4: a,b) 0 day; c,d) 3 days; e,f) 7 days; g,h) 14 days; and i,j) 21 days.

Fig. 5 presents the micrographs of the surface of the pellets of the HAp/TCP@ZnO composite after different contact times with the SBF solution. The indication of bioactive material consists of apatite crystal formation on the sample; in this case, the deposition of apatite on the material surface was more evident after 7 days of contact with the SBF (Figs. 5e and 5f). However, crystal precipitation increased as the immersion time increased, as can be noticed in Figs. 5g and 5h, after 14 days of testing. Complementing the observation of the morphology after crystal deposition, an energy dispersive spectroscopy (EDS) analysis was performed: Figs. 6a and 6b, respectively, for the samples shown in Fig. 5h (14 days) and Fig. 5j (21 days). In this case, the qualitative chemical analysis confirmed the presence of the characteristic elements of apatite, namely phosphorus (P), calcium (Ca), and oxygen. Zinc (Zn) present on its surface was also detected, given the addition of ZnO,

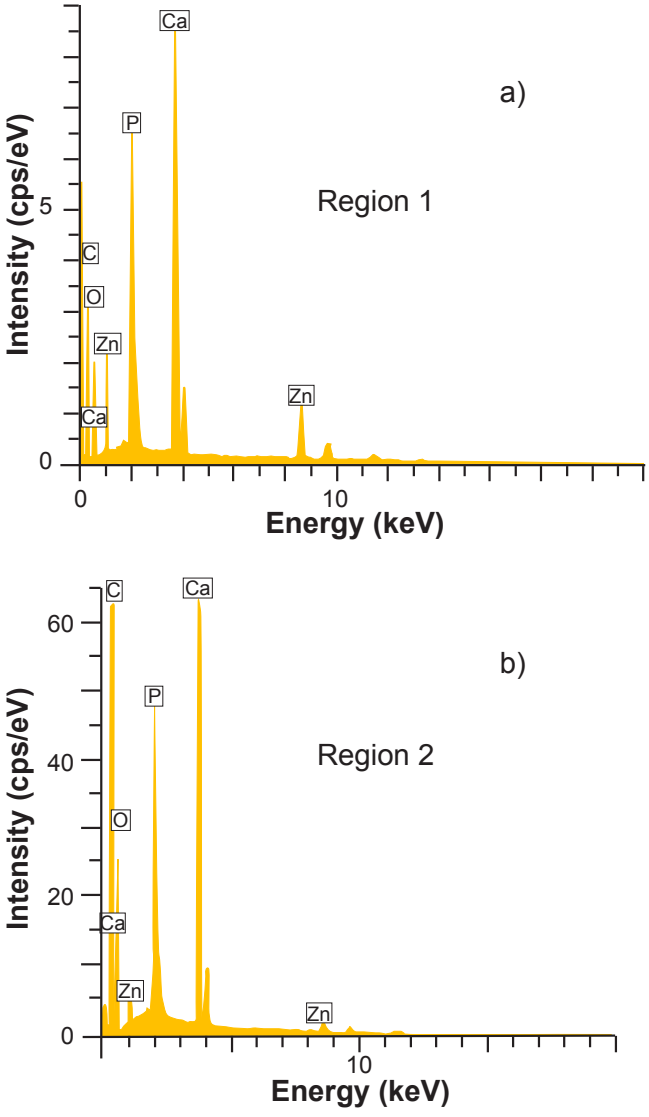

Figure 6: EDS spectra of the surfaces of HAp/TCP@10%ZnO composite samples after: a) 14 days (region 1, Fig. 5h); and b) 21 days (region 2, Fig. 5j).

and carbon (C) was attributed to the tape used in the test. We also point out that Zn^{2+} ions stimulate bone growth and, therefore, contribute to the bioactivity of a material [27]. According to the *in vitro* studies performed by Seo et al. [28], the presence of Zn increases the proliferation of bone cells. Hence, the presence of ZnO in the studied composite not only added antimicrobial properties to it but also increased its bioactivity.

CONCLUSIONS

A biocomposite based on hydroxyapatite, tricalcium phosphate, and zinc oxide nanoparticles was successfully produced. Based on the characterizations performed, it was confirmed that this composite has properties of high interest for applications as a bone substitute, given that its constituent materials displayed chemical similarities with bones and suggested a high bioactivity. Hemolysis tests confirmed its non-toxicity and the antimicrobial assay demonstrated activity against S. aureus bacteria. Hence, we conclude that the present composite has the potential to be a material for bone regeneration.

REFERENCES

[1] Research and Markets, "Global orthopedic surgery market report" (2018).
[2] C. Gao, S. Peng, P. Feng, C. Shuai, Bone Res. **5** (2017) 17059.
[3] H.M. Júnior, C.F. Beltrão, J.C. Furlani, F. Kassardjian, L.R. Mugayar, W.J. Genovese, Rev. Ass. Paul. Cir. Dent. **70** (2016) 198.
[4] M.A.T. Aroni, P.F.C. Neto, G.J.P. Oliveira, R.A.C. Marcantoni, E.M. Junior, Braz. J. Implantol. Heath Sci. **2**, 9 (2020) 28.
[5] Y.C. Huang, C.Y. Chen, K.C. Lin, J.H. Renn, Y.W. Tarng, C.J. Hsu, W.N. Chang, S.W. Yang, J. Orthop. Surg. Res. **13**, 1 (2018) 115.
[6] R. Šćepanović, M. Stevanović, Ser. J. Exp. Clin. Res., *in print*.
[7] G.F. De Grado, L. Keller, Y. Idoux-Gillet, Q. Wagner, A.M. Musset, N.B. Jessel, F. Bornet, D. Ofnner, J. Tissue Eng. **4** (2018) 1.
[8] M. Gutierres, M.A. Lopes, N.S. Hussain, A.T. Cabral, L. Almeida, J.D. Santos, Arq. Med. **19** (2006) 153.
[9] J. Jeong, J.H. Kim, J.H. Shim, N.S. Wang, C.Y. Heo, Biomater. Res. **23** (2019) 4.
[10] J.P. O'Connor, D. Kanjilal, M. Teitelbaum, S.S. Lin, J.A. Cottrell, Materials **13**, 10 (2020) 2211.
[11] Y. Qiao, W. Zhang, P. Tian, F. Meng, H. Zhu, X. Jiang, X. Liu, P.K. Chu, Biomaterials **35**, 25 (2014) 6882.
[12] A. Sirelkhatim, S. Mahmud, A. Seeni, N.H.M. Kaus, L.C. Ann, S.K.M. Bakhori, H. Hasan, D. Mohamad, Nanomicro Lett. **7**, 3 (2015) 219.
[13] A.A. Barbosa, A.S. Júnior, A.V. Ferraz, J. Mater. Res. **34**, 11 (2019) 1922.
[14] C.A. Martinez, U. Gilabertc, L. Garrido, M. Rosenbusch, A. Ozóis, Proc. Mater. Sci. **9** (2015) 484.
[15] W.B. dos Santos, A.M.G. Silva, J.C. da Silva, T.H.L. Bernardo, B.M.L. de Assis, R.C.S.S. Veríssimo, Rev. SOBECC **21**, 1 (2016) 46.
[16] T. Kokubo, H. Takadama, Biomaterials **27** (2006) 2907.
[17] NCCLS, "Performance standards for antimicrobial disk susceptibility tests", 8th ed., Wayne (2003).
[18] P.M. Narayanan, W.S. Wilson, A.T. Abraham, M. Sevanan, BioNanoScience **2**, 4 (2012) 329.
[19] S. Albukhaty, H. Al-Karagoly, M.A. Dragh, J. Biotech. Res. **1** (2020) 47.
[20] B. Abebe, E.A. Zereffa, A. Tadesse, H.C.A. Murthy, Nanoscale Res. Lett. **15** (2020) 1.
[21] S.V. Oliveira, S.N. Cavalcanti, G.P. Rabello, E.M. Araújo, M.V.L. Fook, in VI Congr. Nac. Eng. Mec., Campina Grande (2010).
[22] A. Becheri, M. Durr, P.L. Nostro, P. Baglione, J. Nanopartic. Res. **4** (2008) 679.
[23] M. Gusatti, G.S. Barroso, C.E. Campos, D.A.R. de Souza, J.A. do Rosário, R.B. Lima, Mater. Res. **2** (2010) 264.
[24] B. Priyadarshini, U. Anjaneyulu, U. Vijalakshmi, Mater. Des. **119** (2017) 446.
[25] K.P. Tank, K.S. Chudasama, V.S. Thaker, M.J. Joshi, J. Crystal Growth **401** (2014) 474.
[26] S.S. Bandgar, H.M. Yadav, S.S. Shirguppikar, M.A. Shinde, R.V. Shejawal, J. Korean Ceram. Soc. **54**, 2 (2017) 158.
[27] M. Yamaguchi, Mol. Cell. Biochem. **11** (1998) 119.
[28] H.J. Seo, Y.E. Cho, T. Kim, H.J. Seo, Y.E. Cho, K. Taewan, Nutr. Res. Pract. **4**, 5 (2010) 356.
(Rec. 08/09/2022, Rev. 30/11/2022, 13/02/2023, Ac. 23/02/2023)

(cc) BY-NC